Supplementary Information

A simple model for poration induced electro deformation of Giant Vesicles

Rochish M. Thaokar*[a], Rupesh Kumar[b], Nalinikanta Behera[c], and Mohammad Maoyafikuddin[d]

[a,c] *Department of Chemical Engineering, Indian Institute of Technology Bombay, Mumbai 400076, Maharashtra, India. E-mail: rochish@che.iitb.ac.in*
[b,d] *Centre for Research in Nanotechnology & Science, Indian Institute of Technology Bombay, Mumbai 400076, Maharashtra, India.*

S1 Image analysis

The images of deformed Giant Unilamellar Vesicles (GUVs) were extracted from the study published by Maoyafikuddin et al. (2025)[1]. These images were analyzed using ImageJ software. Initially, the outlines of the deformed GUVs were drawn using the freehand selection tool in ImageJ, and the selections were added to the Region of Interest (ROI) manager. To determine the centroid of each ROI, the following steps were taken: Navigate to Analyze > Set Measurements, select the 'Centroid' option, and click 'OK'. Select the ROI, then go to Analyze > Measure; a window will pop up displaying the centroid coordinates. Subsequently, the origin was redefined to align with the centroid coordinates by accessing 'Edit > Selection > Properties' and inputting the centroid's X and Y values as the new origin for the selected ROI. This adjustment ensures that the extracted coordinates are referenced from the centroid. After setting the new origin, the ROI's coordinates were extracted by selecting 'List Coordinates' in Imagej> Edit> Selection > Properties dialogue. For scenarios requiring the extraction of a specific number of coordinates or integration with Python-based analyses, a custom macro was developed to retrieve the coordinates and format them as a NumPy array.

// Define origin offset if necessary (set to 0 if not needed) x0 = 39.829; y0 = 42.344;

// Get ROI coordinates getSelectionCoordinates(x, y); n = x.length; desiredPoints = 500

// Create strings for NumPy arrays $xString = "x_ex = np.array([";$ $yString = "y_ex = np.array([";$

// Loop over desired points and interpolate linearly between ROI points for (i = 0; i < desiredPoints; i++) u = i * (n / desiredPoints); idx1 = floor(u); idx2 = (idx1 + 1) t = u - idx1;

// Linear interpolation, then adjust by subtracting origin offset if needed xi = (1 - t) * x[idx1] + t * x[idx2] - x0; yi = (1 - t) * y[idx1] + t * y[idx2] - y0;

// Append to strings with proper formatting if(i < desiredPoints - 1) xString += " " + xi + ", "; yString += " " + yi + ", "; else xString += " " + xi; yString += " " + yi; xString += "])"; yString += "])"; // Print the NumPy array formatted strings print(xString); print(""); print(yString);

After extracting the coordinates of the deformed Giant Unilamellar Vesicles (GUVs) using ImageJ, the radial deformation parameters were determined by fitting the experimental data to a theoretical model. This involved minimizing the difference between the experimentally obtained radial distances and those predicted by the following equation:

$$r(\theta) = r + S_2 \cdot \frac{3\cos^2\theta - 1}{2} + S_4 \cdot \frac{3 - 30\cos^2\theta + 35\cos^4\theta}{8} + S_6 \cdot \frac{-5 + 105\cos^2\theta - 315\cos^4\theta + 231\cos^6\theta}{16}$$

Here, $r(\theta)$ represents the normal radial distance of the membrane surface at angle θ, r is the normalised radius, and S_2, S_4, and S_6 are deformation coefficients respectively. The optimisation was performed using Python's numerical libraries to minimise the radial distance between the experimental and theoretical coordinates, thereby accurately determining the values of r, S_2, S_4, and S_6 for available experimental deform images.

Figures S1,S2,S3, and S4 show the coordinated extraction of deformed shapes (blue continuous) and the theoretically fitted shape (red circle).

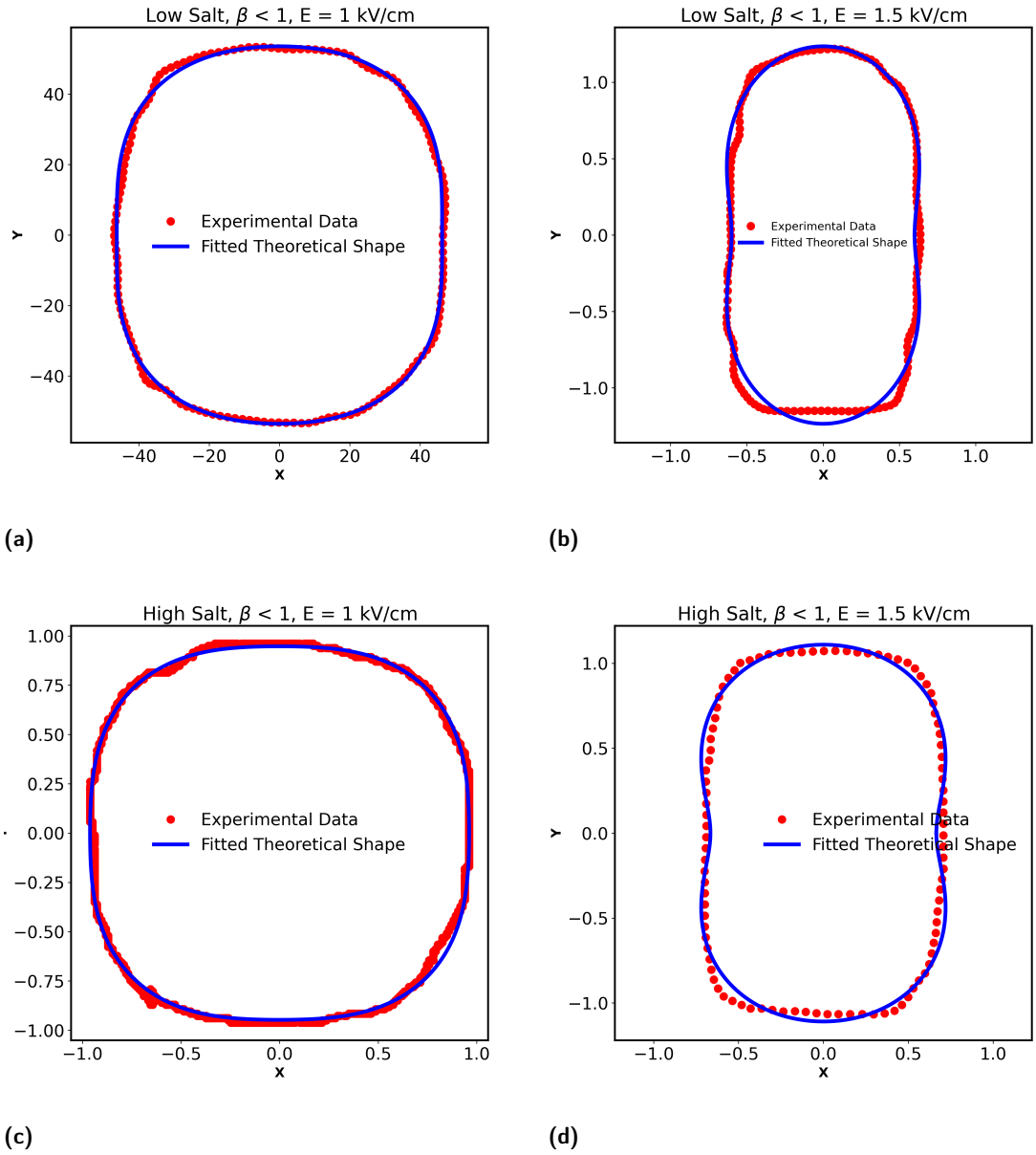

Fig. S1 Experimental coordinates of images of deform vesicles (red circle) and fitted theoretical shapes (blue continuous lines) are shown for the four cases of $\beta < 1$.

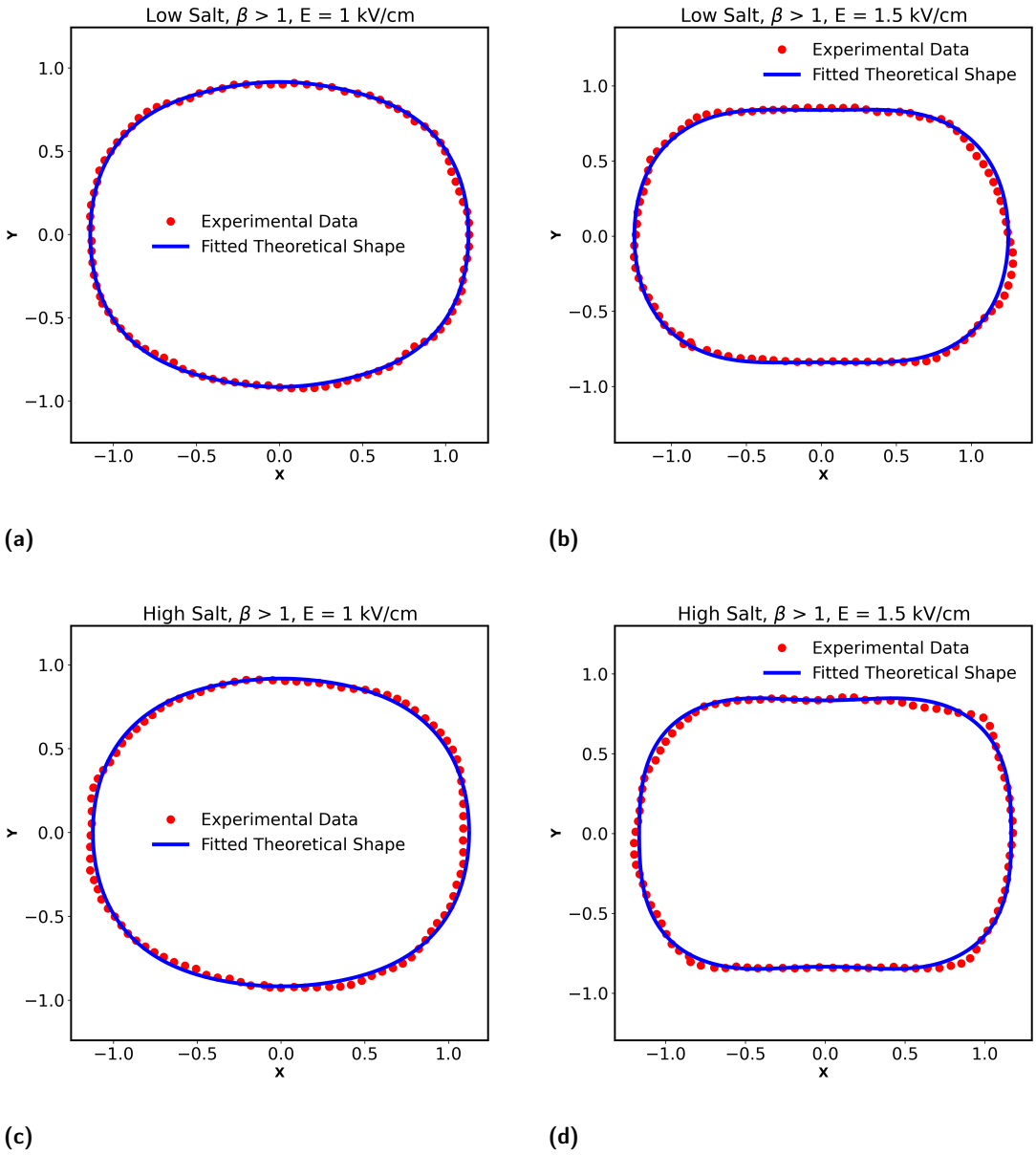

Fig. S2 Experimental coordinates of images of deformed vesicles (red circle) and fitted theoretical shapes (blue continuous lines) are shown for the four cases of $\beta > 1$.

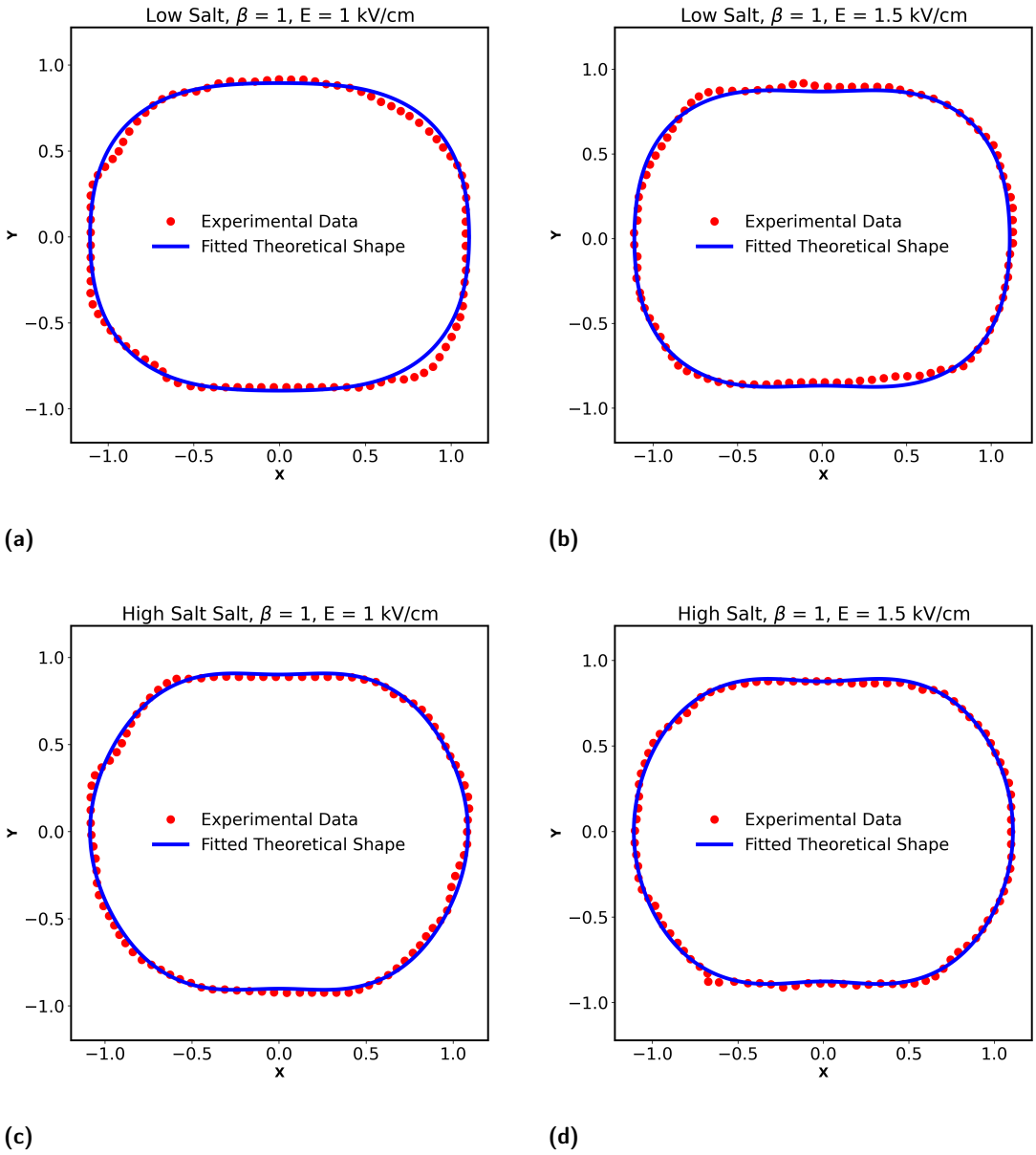

Fig. S3 Experimental coordinates of deform images of deform vesicles (red circle) and fitted theoretical shapes (blue continuous lines) are shown for the four cases of $\beta = 1$.

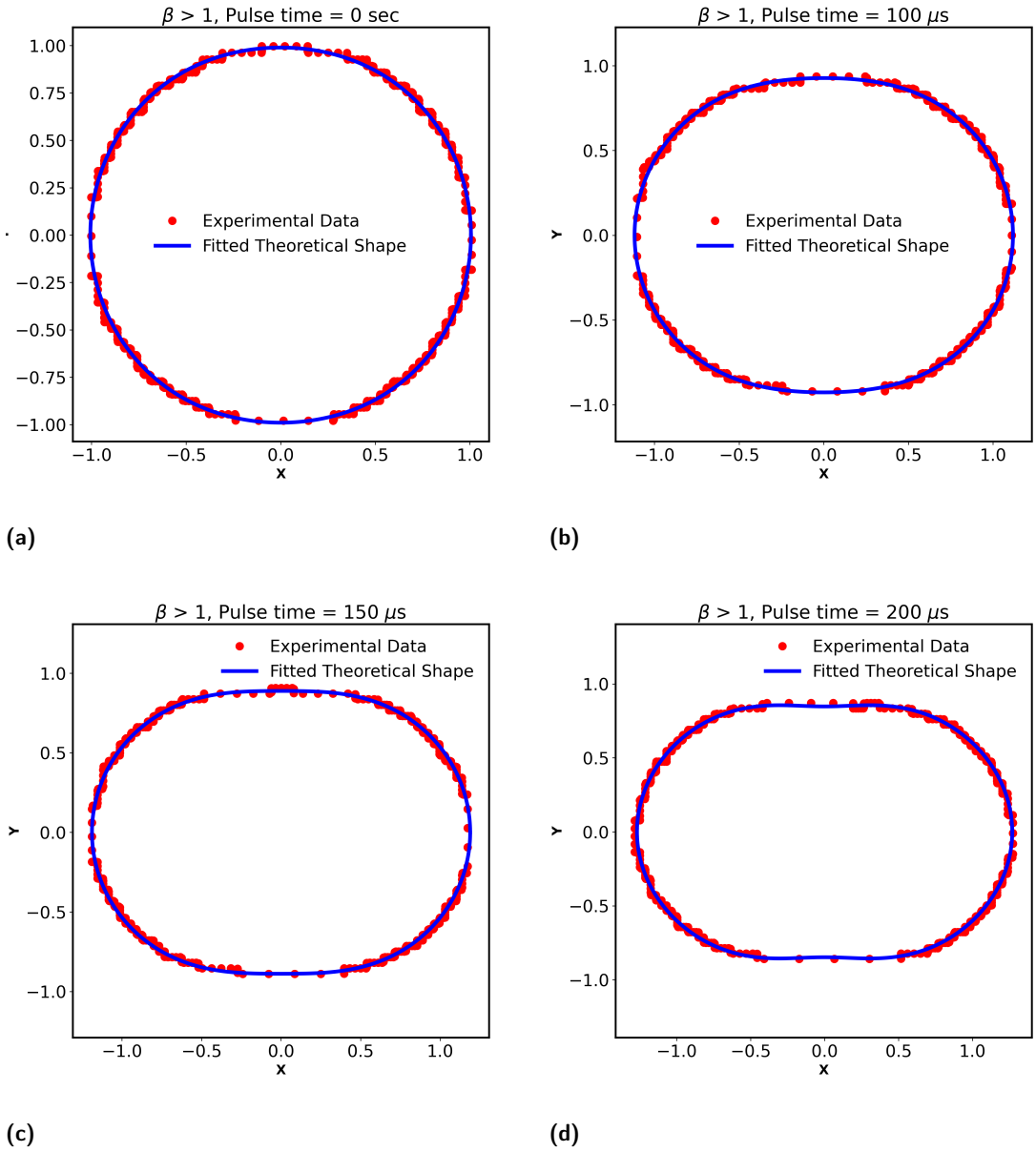

Fig. S4 Experimental coordinates of images of a deformed vesicle (red circle) and fitted theoretical shapes (blue continuous lines) are shown for the cases in figure 3A of Karin A. Riske and Rumiana Dimova (2006)[2]. Tubelike deformation of a vesicle of R = 24.1 μm at conductivity conditions $\beta = 1.38$, $\sigma_{in} = 16.5$ μS/cm, $\sigma_{out} = 12$ μS/cm, $c_{in} = 0.1$ mM NaCl, and $c_{out} = 0.05$ mM NaCl. The pulse parameters are E = 2 kV/cm and $t_p = 200$ μs. Adapted from Riske and Rumiana Dimova (2006)[2].

S2 Validation of results of Salipante and Vlahovska

We validate the code for the non-conducting membrane, Ge(t) = 0, and use the data for the two-pulse protocol suggested by Salipante and Vlahovska[3] in their figure 9. The oblate shape at the end of the short strong pulse and the prolate shape at long times, during the extended weak pulse, as predicted by the entropic model for the unporated vesicle, are shown, together with the variation of AR vs time. The variation of TMP and shape parameters with time are provided. Good agreement is observed between the prediction of our code and the data presented in[3].

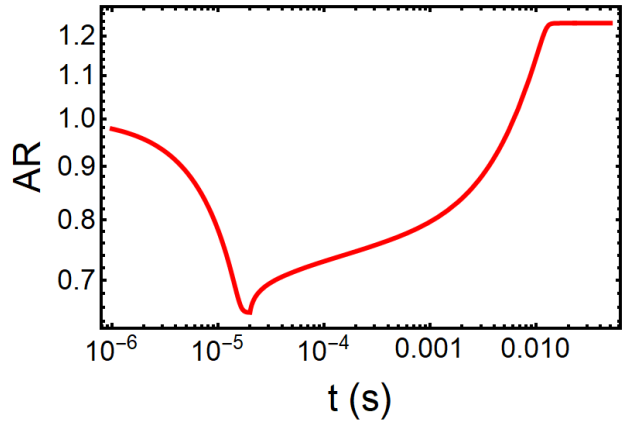

(a) AR vs time, showing oblate deformation followed by recovery to prolate shape

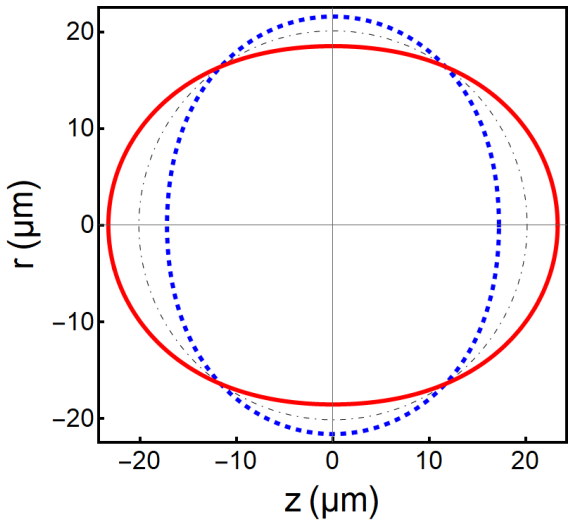

(b) Shapes at t=0μs black dot dashed, t=10 μs blue dashed, t=50 ms red solid.

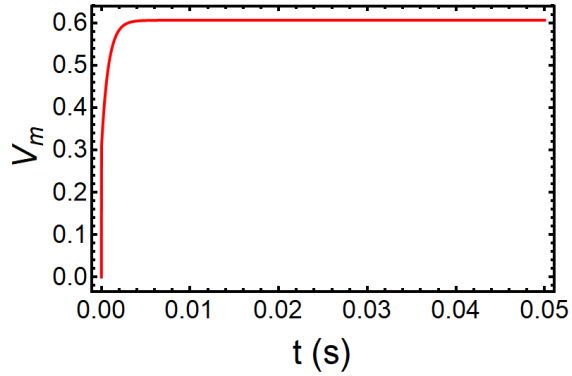

(c) TMP (V_m) vs time

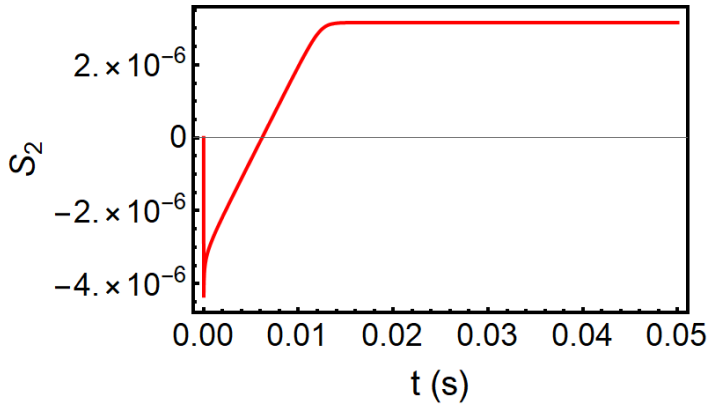

(d) S_2 vs time

Fig. S5 Validation of Salipante and Vlahovska[3] (Figure 9a) by the present model: $R_o = 20.2\ \mu m$, $C_m = 0.007\ F/m^2$, $\sigma_{in} = 2\ \mu S/cm$, $\sigma_{ex} = 10\ \mu S/cm$, $\gamma_{ini} = 4 \times 10^{-7}\ N/m$. Showing oblate deformation at the end of short pulse $(10\ \mu s)$ and prolate deformation at the end long pulse $(50\ ms)$. The oblate shape at the end of the short strong pulse and the prolate shape at long times, during the extended weak pulse, as predicted by the entropic model for the unporated vesicle, are shown, together with the variation of AR vs time. The variation of TMP and shape parameters with time.

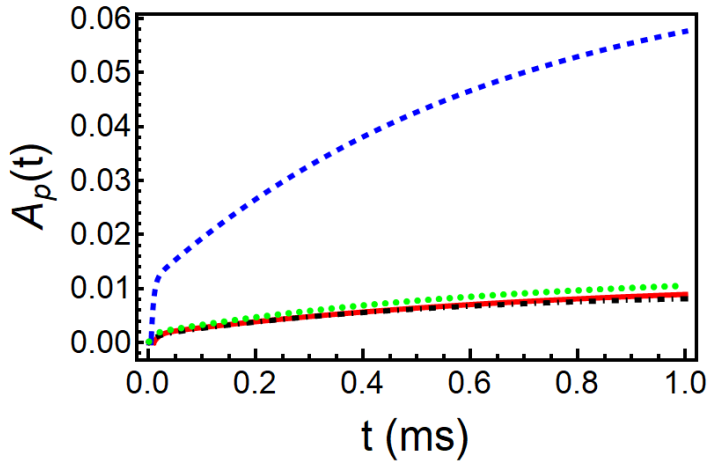

(a) $\beta < 1$

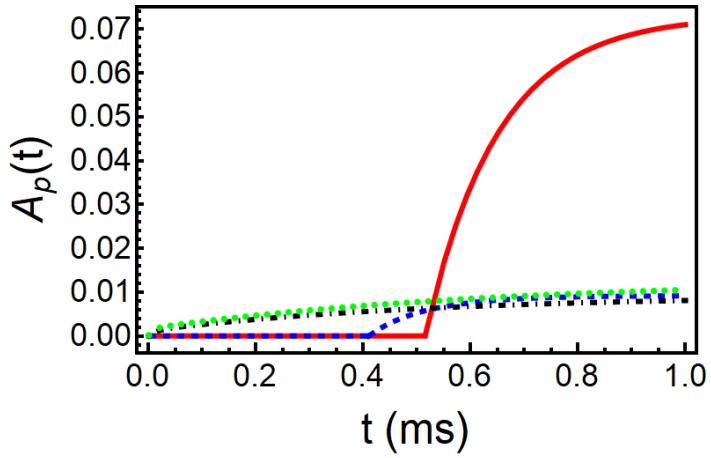

(b) $\beta = 1$

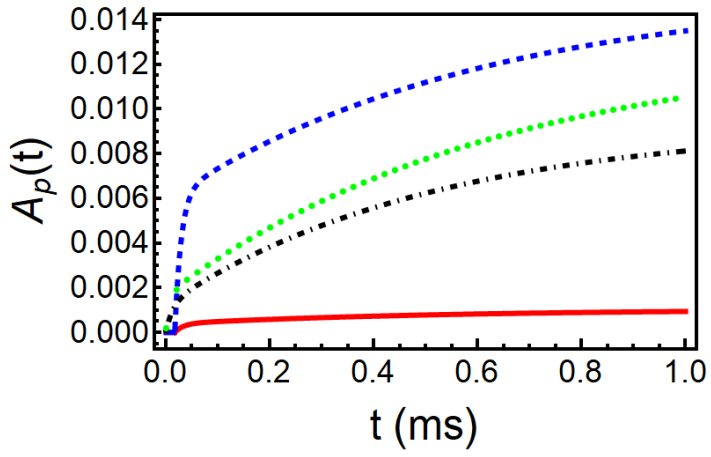

(c) $\beta > 1$

Fig. S6 The fractional pore area data plotted with parameters in using the electroporation model. 1 kV/cm, low salt- solid line (red), 1.5 kV/cm, low salt- dashed (blue), 1 kV/cm, high salt- dot dashed (black), and 1.5 kV/cm, high salt- dotted (green) in all three cases (a) $\beta < 1$, (b) $\beta = 1$, and (c) $\beta > 1$.

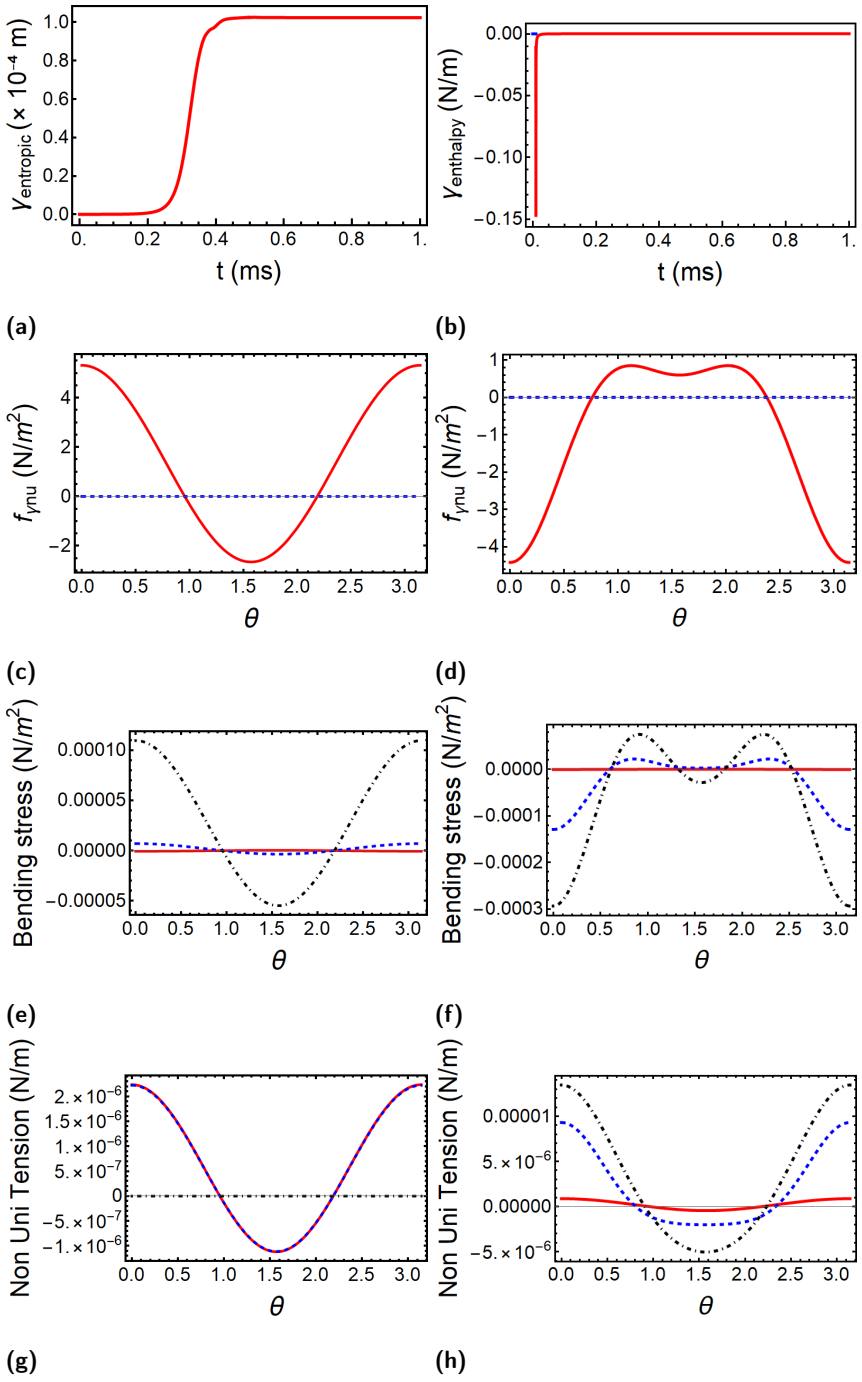

Fig. S7 Plots for $\beta < 1$, low salt: First column E=1 kV/cm, unporated, second column E=1 kV/cm, porated. (a) and (b) $\gamma_{entropic}$ and $\gamma_{enthalpy}$ vs t plot, (c) and (d) Capillary stress due to non uniform tension ($f_{\gamma nu}$) vs t, (e) and (f) Bending stress vs θ, $t = \tau_c/2$-red solid, $t = 1.5\tau_c$-blue dashed, $t = t_p$-black dotdashed, (g), and (h) Non Uniform tension (τ_n^e) vs θ, $t = \tau_c/2$-red solid, $t = 1.5\tau_c$ -blue dashed, $t = t_p$-black dotdashed.

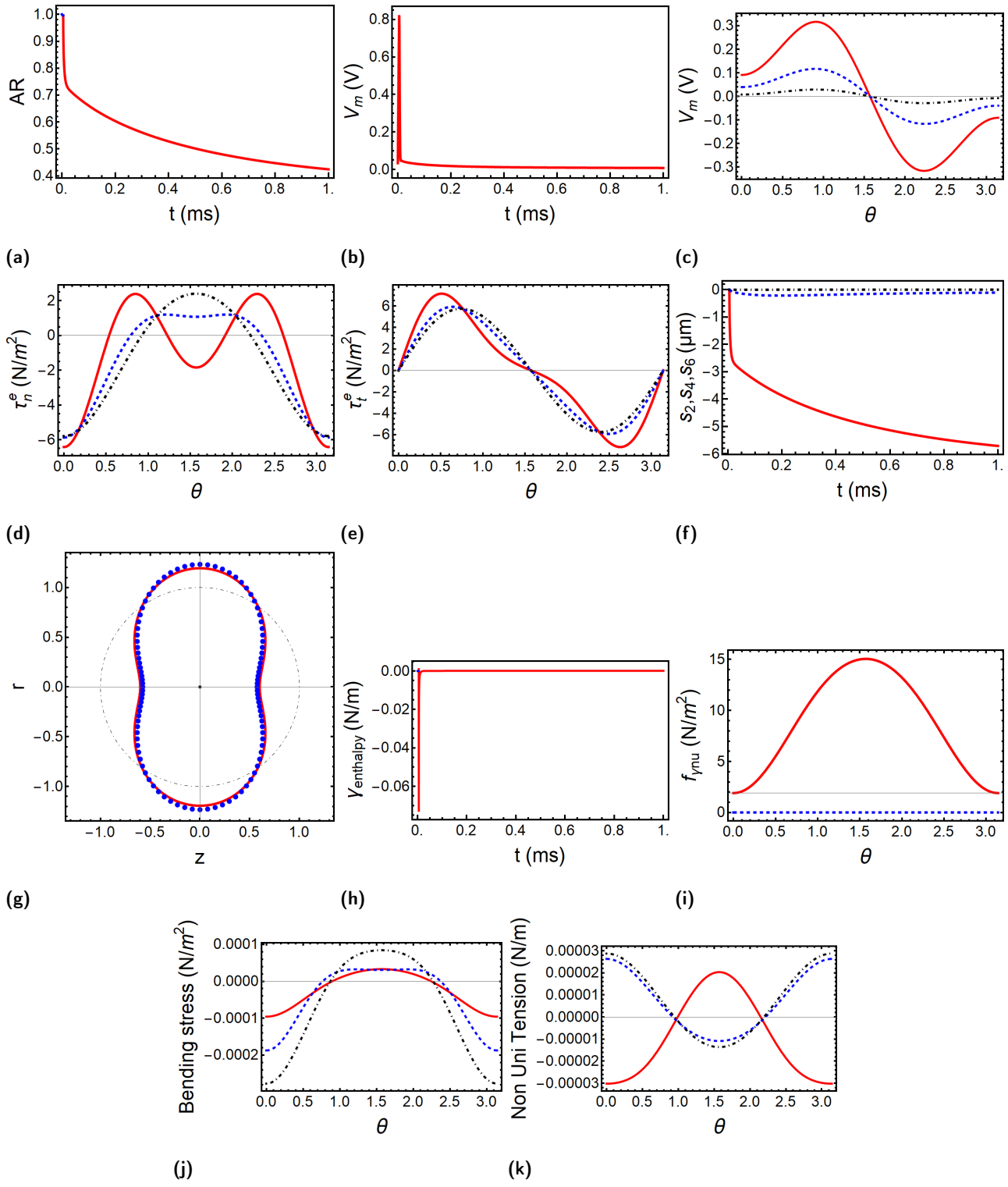

Fig. S8 Plots for $\beta < 1$, low salt, E=1.5 kV/cm, porated: (a) AR vs t plot, (b) V_{mb} vs t, (c) V_{mb} vs θ, $t = \tau_c/2$-red solid, $t = 1.5\tau_c$-blue dashed, $t = t_p$-black dotdashed, (d) Normal electric stress (τ_n^e) vs θ, $t = \tau_c/2$-red solid, $t = 1.5\tau_c$ -blue dashed, $t = t_p$-black dotdashed, (e) Tangential electric stress (τ_t^e) vs θ, $t = \tau_c/2$-red Solid, $t = 1.5\tau_c$-blue dashed, $t = t_p$-black dotdashed, (f) s_2, s_4, s_6 vs t, electric field directed from left to right, s_2-red solid, s_4-blue dashed, s_6-black dotdashed, (g) r vs z circle- black dotdashed, model prediction-red solid, experimental - blue dots (h) $\gamma_{enthalpy}$ vs t plot, (i) Capillary stress due to non uniform tension ($f_{\gamma nu}$) vs t, (j) Bending stress vs θ, $t = \tau_c/2$-red solid, $t = 1.5\tau_c$-blue dashed, $t = t_p$-black dotdashed, (k) Non Uniform tension (τ_n^e) vs θ, $t = \tau_c/2$-red solid, $t = 1.5\tau_c$ -blue dashed, $t = t_p$-black dotdashed.

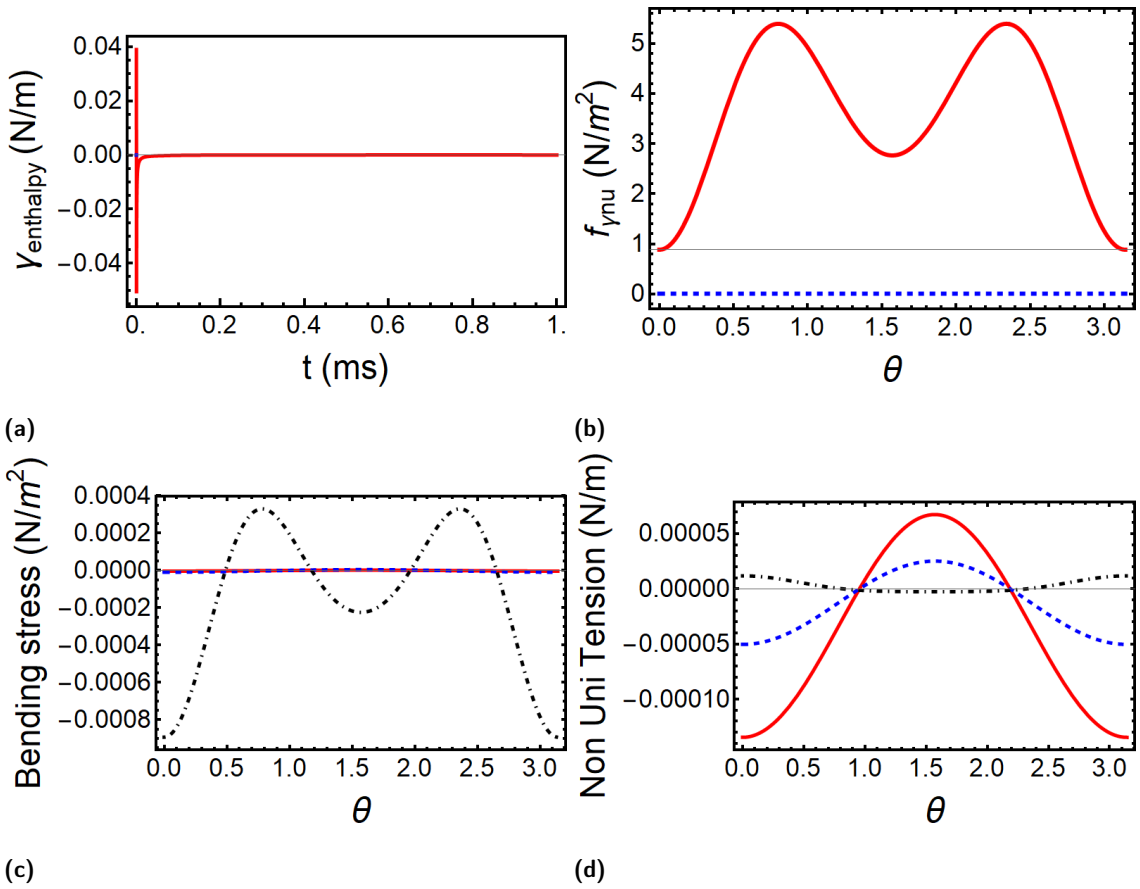

Fig. S9 Plots for $\beta < 1$, high salt, E=1 kV/cm, porated: (a) $\gamma_{enthalpy}$ vs t plot, (b) Capillary stress due to non uniform tension ($f_{\gamma nu}$) vs t, (c) Bending stress vs θ, $t = \tau_c/2$-red solid, $t = 1.5\tau_c$-blue dashed, $t = t_p$-black dotdashed, (d) Non Uniform tension (τ_n^e) vs θ, $t = \tau_c/2$-red solid, $t = 1.5\tau_c$ -blue dashed, $t = t_p$-black dotdashed.

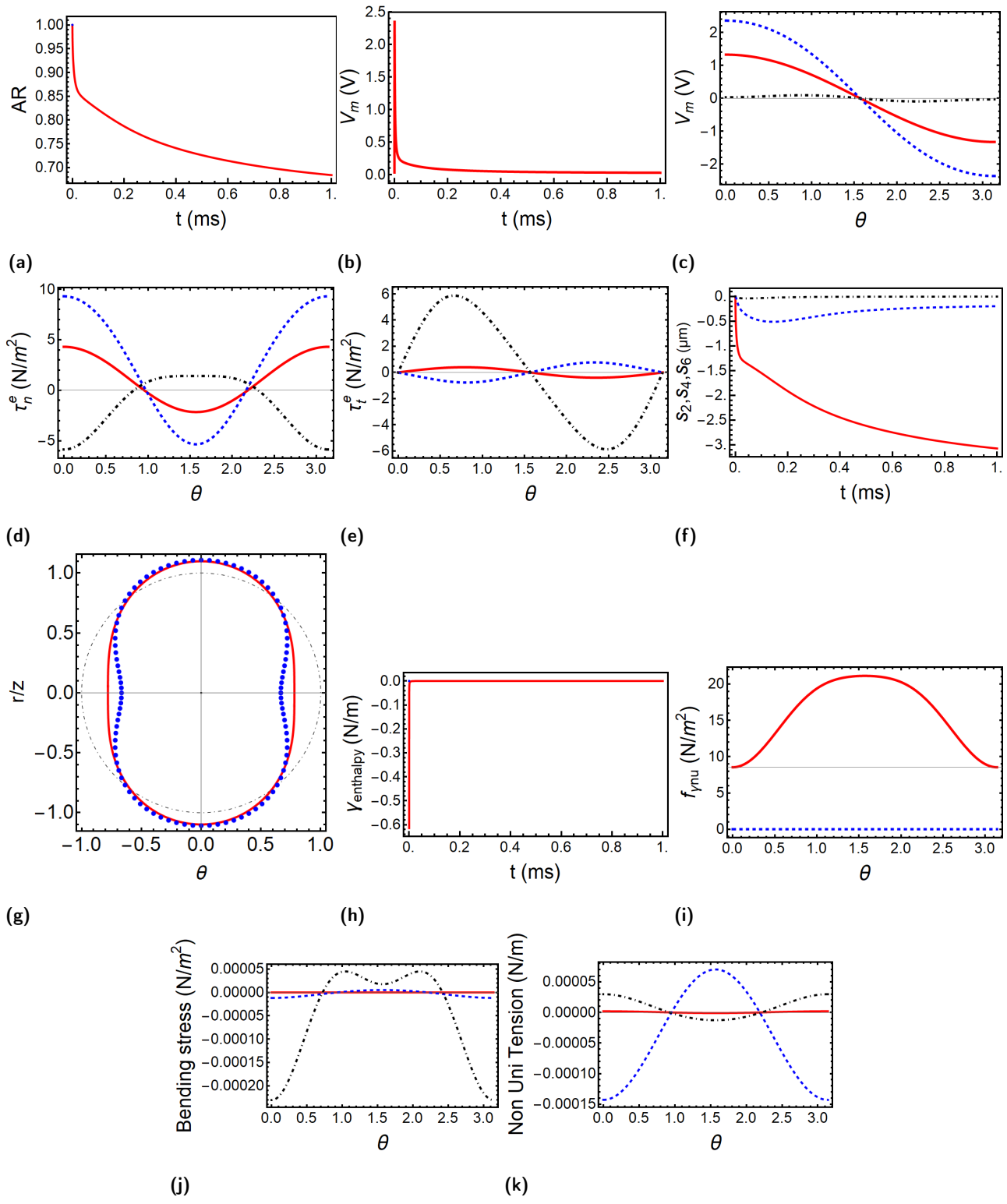

Fig. S10 Plots for $\beta < 1$, high salt, E= 1.5 kV/cm, porated:(a) AR vs t plot, (b) V_{mb} vs t, (c) V_{mb} vs θ, $t = \tau_c/2$-red solid, $t = 1.5\tau_c$-blue dashed, $t = t_p$-black dotdashed, (d) Normal electric stress (τ_n^e) vs θ, $t = \tau_c/2$-red solid, $t = 1.5\tau_c$ -blue dashed, $t = t_p$-black dotdashed, (e) Tangential electric stress (τ_t^e) vs θ, $t = \tau_c/2$-red Solid, $t = 1.5\tau_c$-blue dashed, $t = t_p$-black dotdashed, (f) s_2, s_4, s_6 vs t, s_2-red solid, s_4-blue dashed, s_6-black dotdashed, (g) r vs z circle- black dotdashed, model prediction-red solid, experimental - blue dots (h) $\gamma_{enthalpy}$ vs t plot, (i) Capillary stress due to non uniform tension ($f_{\gamma nu}$) vs t, (j) Bending stress vs θ, $t = \tau_c/2$-red solid, $t = 1.5\tau_c$-blue dashed, $t = t_p$-black dotdashed, (k) Non Uniform tension (τ_n^e) vs θ, $t = \tau_c/2$-red solid, $t = 1.5\tau_c$ -blue dashed, $t = t_p$-black dotdashed.

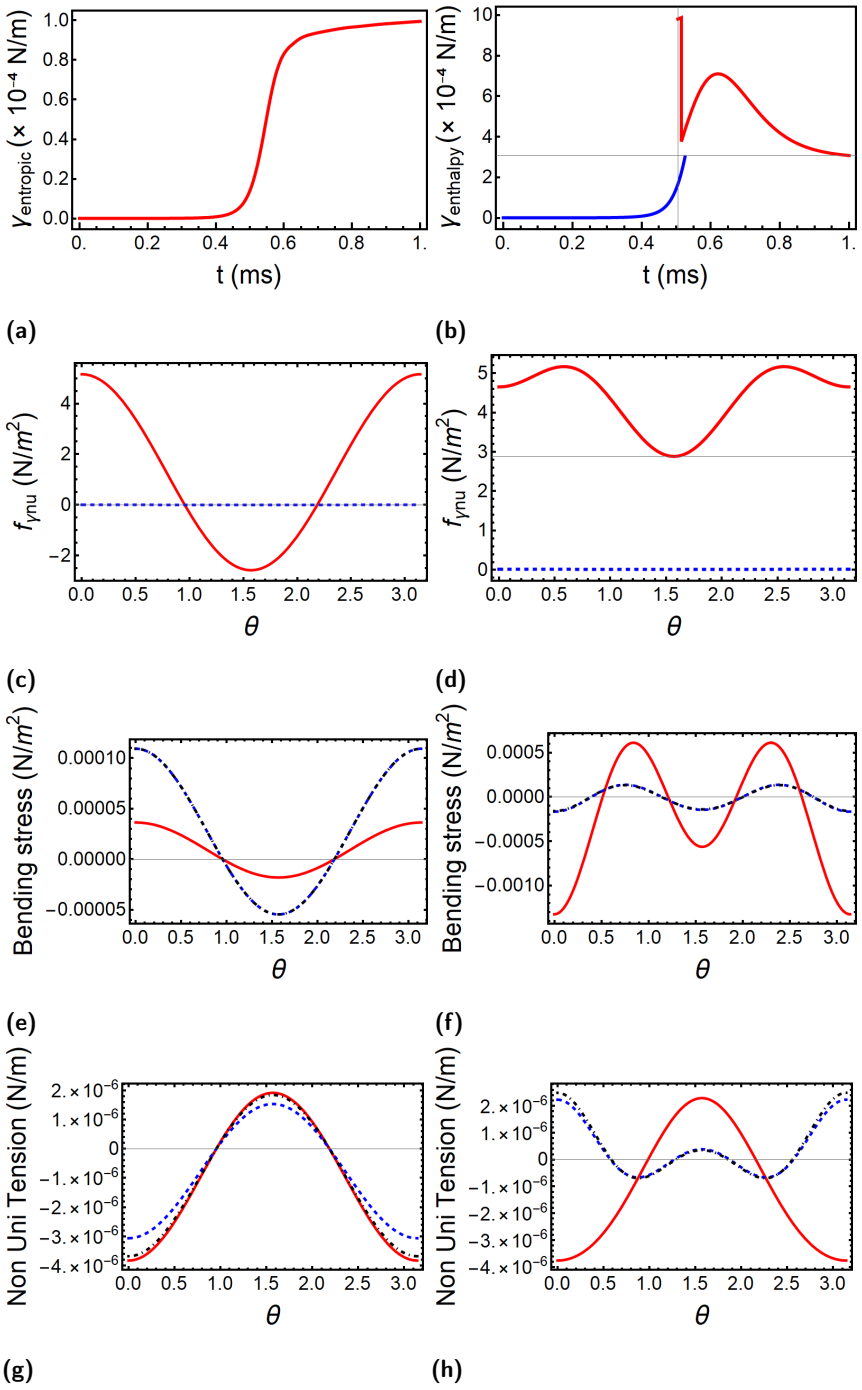

Fig. S11 Plots for $\beta = 1$, low salt: First column E=1 kV/cm, unporated, second column E=1 kV/cm, porated. (a) and (b) $\gamma_{entropic}$ and $\gamma_{enthalpy}$ vs t plot, (c) and (d) Capillary stress due to non uniform tension ($f_{\gamma nu}$) vs t, (e) and (f) Bending stress vs θ, $t = \tau_c/2$-red solid, $t = 1.5\tau_c$-blue dashed, $t = t_p$-black dotdashed, (g), and (h) Non Uniform tension (τ_n^e) vs θ, $t = \tau_c/2$-red solid, $t = 1.5\tau_c$ -blue dashed, $t = t_p$-black dotdashed.

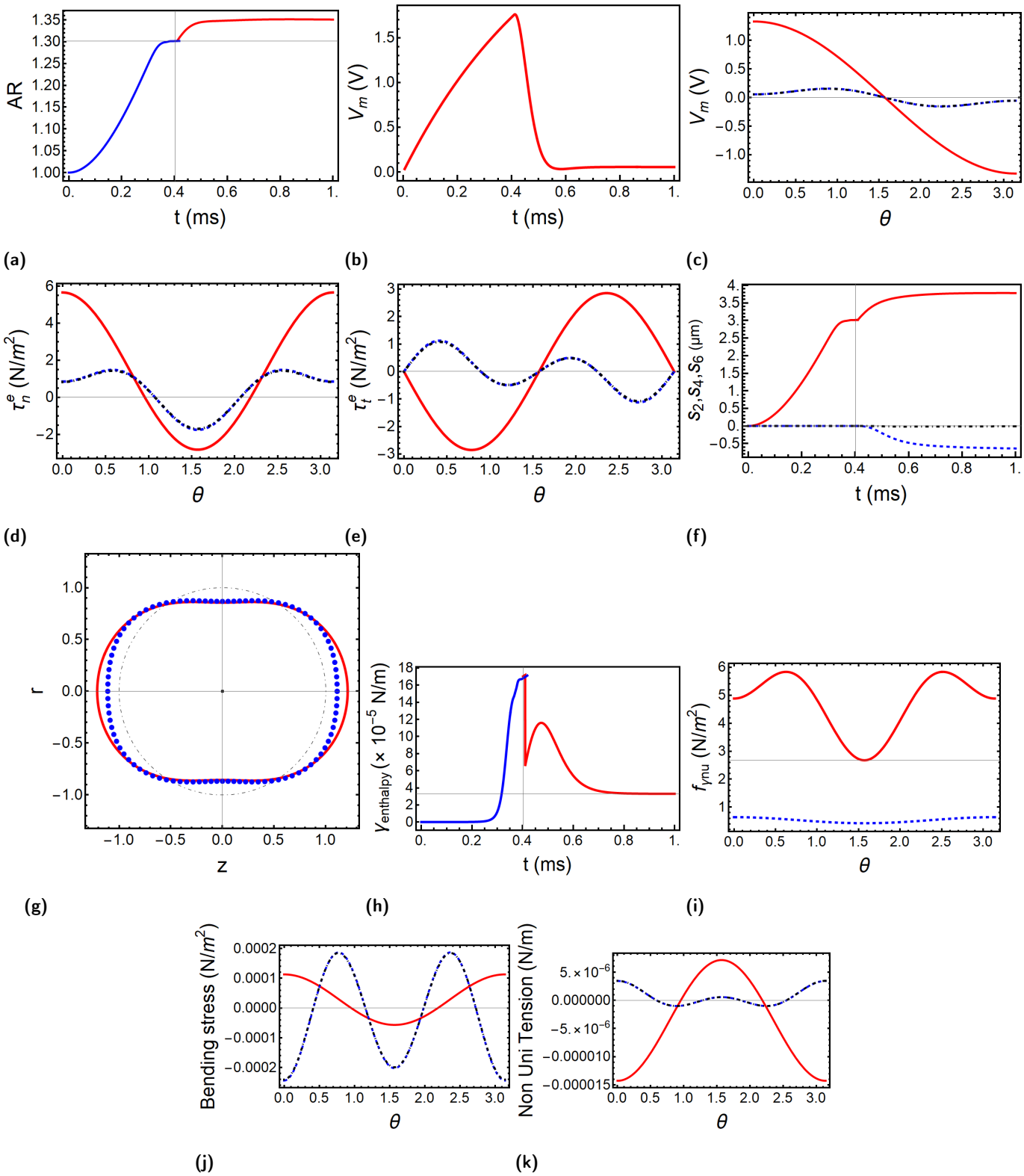

Fig. S12 Plots for $\beta = 1$, low salt, E=1.5 kV/cm, porated: (a) AR vs t plot, (b) V_{mb} vs t, (c) V_{mb} vs θ, $t = \tau_c/2$-red solid, $t = 1.5\tau_c$-blue dashed, $t = t_p$-black dotdashed, (d) Normal electric stress (τ_n^e) vs θ, $t = \tau_c/2$-red solid, $t = 1.5\tau_c$ -blue dashed, $t = t_p$-black dotdashed, (e) Tangential electric stress (τ_t^e) vs θ, $t = \tau_c/2$-red Solid, $t = 1.5\tau_c$-blue dashed, $t = t_p$-black dotdashed, (f) s_2, s_4, s_6 vs t, electric field directed from left to right, s_2-red solid, s_4-blue dashed, s_6-black dotdashed, (g) r vs z circle- black dotdashed, model prediction-red solid, experimental - blue dots (h) $\gamma_{enthalpy}$ vs t plot, (i) Capillary stress due to non uniform tension ($f_{\gamma nu}$) vs t, (j) Bending stress vs θ, $t = \tau_c/2$-red solid, $t = 1.5\tau_c$-blue dashed, $t = t_p$-black dotdashed, (k) Non Uniform tension (τ_n^e) vs θ, $t = \tau_c/2$-red solid, $t = 1.5\tau_c$ -blue dashed, $t = t_p$-black dotdashed.

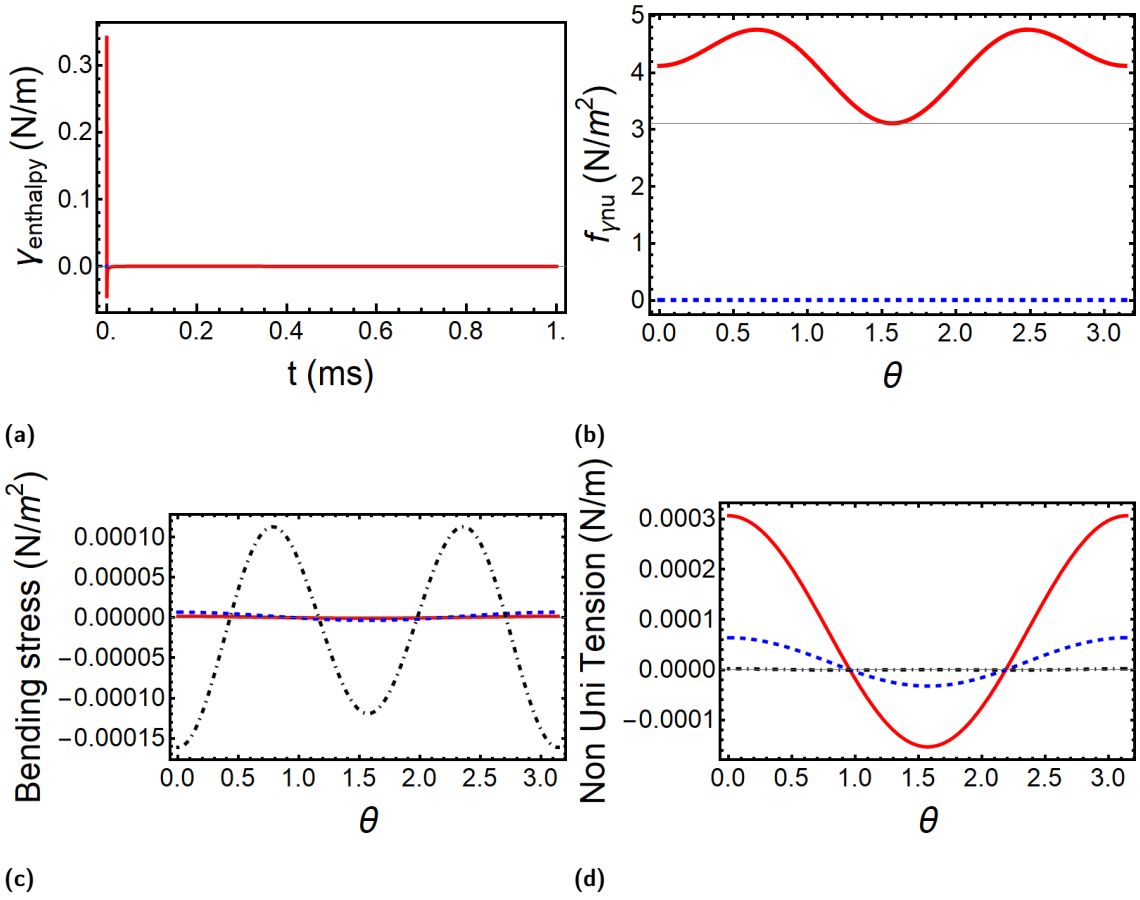

Fig. S13 Plots for $\beta = 1$, high salt, E=1 kV/cm, porated: (a) $\gamma_{enthalpy}$ vs t plot, (b) Capillary stress due to non uniform tension ($f_{\gamma nu}$) vs t, (c) Bending stress vs θ, $t = \tau_c/2$-red solid, $t = 1.5\tau_c$-blue dashed, $t = t_p$-black dotdashed, (d) Non Uniform tension (τ_n^e) vs θ, $t = \tau_c/2$-red solid, $t = 1.5\tau_c$ -blue dashed, $t = t_p$-black dotdashed.

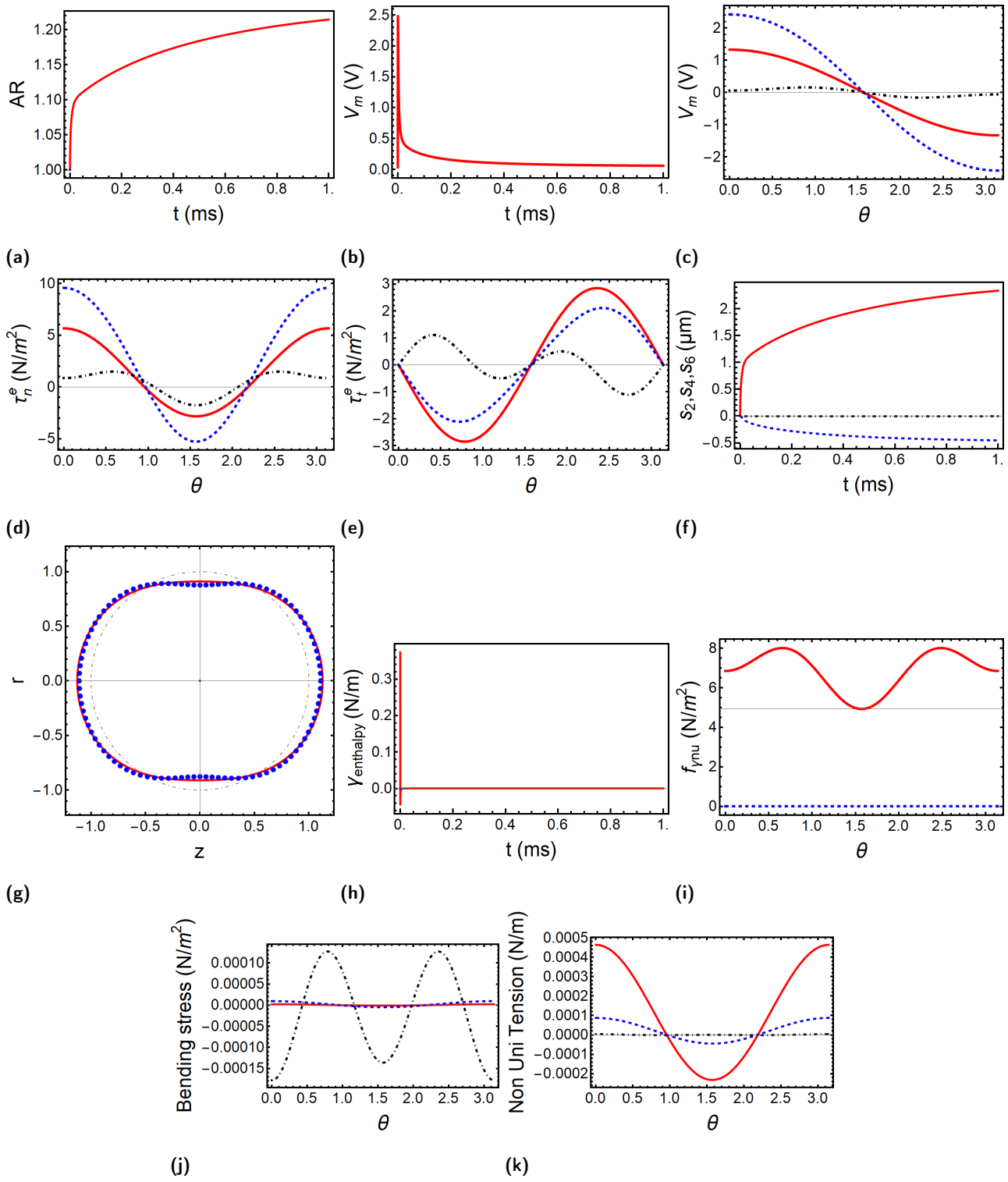

Fig. S14 Plots for $\beta = 1$, high salt, E= 1.5 kV/cm, porated: (a) AR vs t plot, (b) V_{mb} vs t, (c) V_{mb} vs θ, $t = \tau_c/2$-red solid, $t = 1.5\tau_c$-blue dashed, $t = t_p$-black dotdashed, (d) Normal electric stress (τ_n^e) vs θ, $t = \tau_c/2$-red solid, $t = 1.5\tau_c$ -blue dashed, $t = t_p$-black dotdashed, (e) Tangential electric stress (τ_t^e) vs θ, $t = \tau_c/2$-red Solid, $t = 1.5\tau_c$-blue dashed, $t = t_p$-black dotdashed, (f) s_2, s_4, s_6 vs t, s_2-red solid, s_4-blue dashed, s_6-black dotdashed, (g) r vs z circle- black dotdashed, model prediction-red solid, experimental - blue dots (h) $\gamma_{enthalpy}$ vs t plot, (i) Capillary stress due to non uniform tension ($f_{\gamma nu}$) vs t, (j) Bending stress vs θ, $t = \tau_c/2$-red solid, $t = 1.5\tau_c$-blue dashed, $t = t_p$-black dotdashed, (k) Non Uniform tension (τ_n^e) vs θ, $t = \tau_c/2$-red solid, $t = 1.5\tau_c$ -blue dashed, $t = t_p$-black dotdashed.

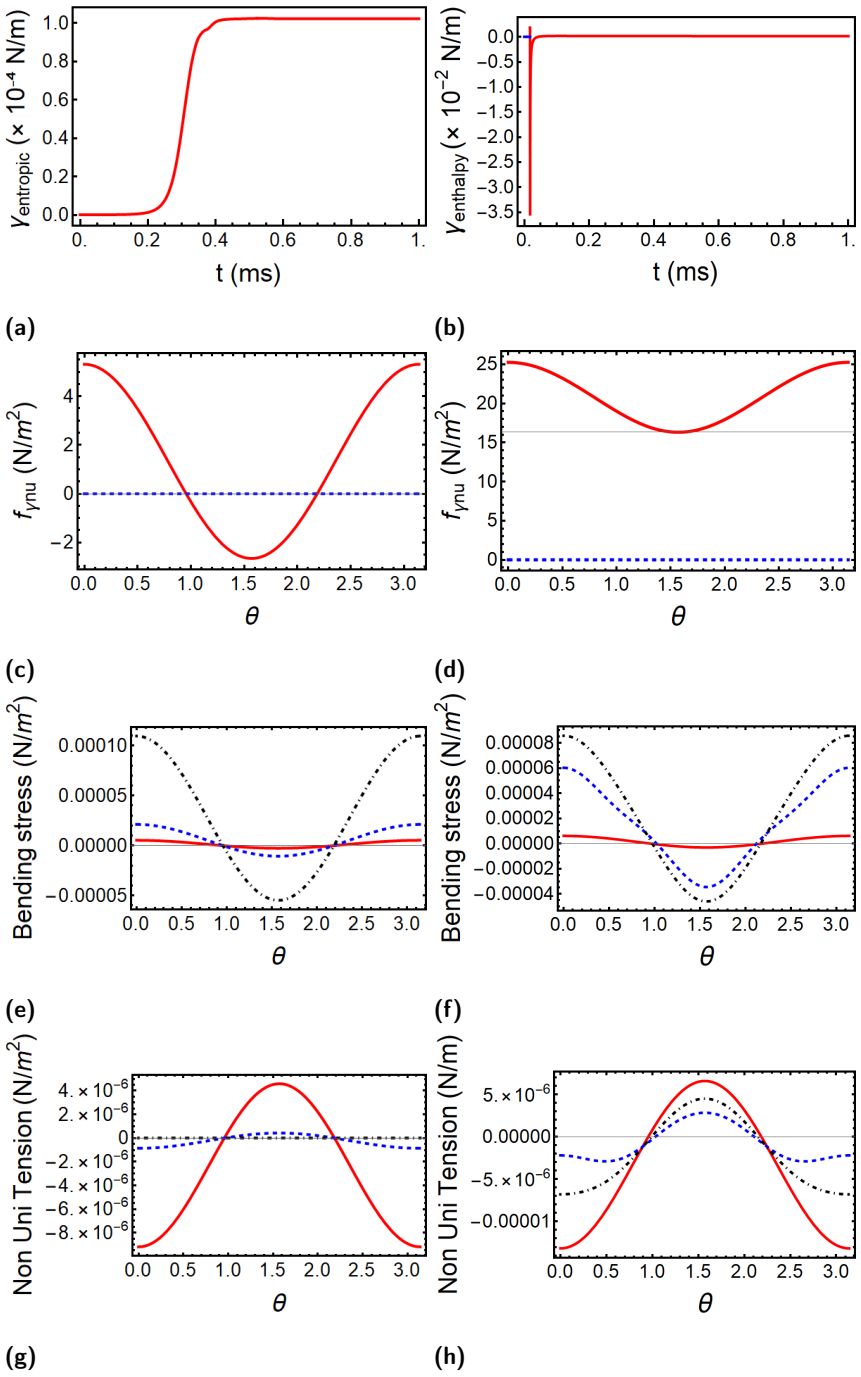

Fig. S15 Plots for $\beta > 1$, low salt: First column E=1 kV/cm, unporated, second column E=1 kV/cm, porated. (a) and (b) $\gamma_{entropic}$ and $\gamma_{enthalpy}$ vs t plot, (c) and (d) Capillary stress due to non uniform tension ($f_{\gamma nu}$) vs t, (e) and (f) Bending stress vs θ, $t = \tau_c/2$-red solid, $t = 1.5\tau_c$-blue dashed, $t = t_p$-black dotdashed, (g), and (h) Non Uniform tension (τ_n^e) vs θ, $t = \tau_c/2$-red solid, $t = 1.5\tau_c$ -blue dashed, $t = t_p$-black dotdashed.

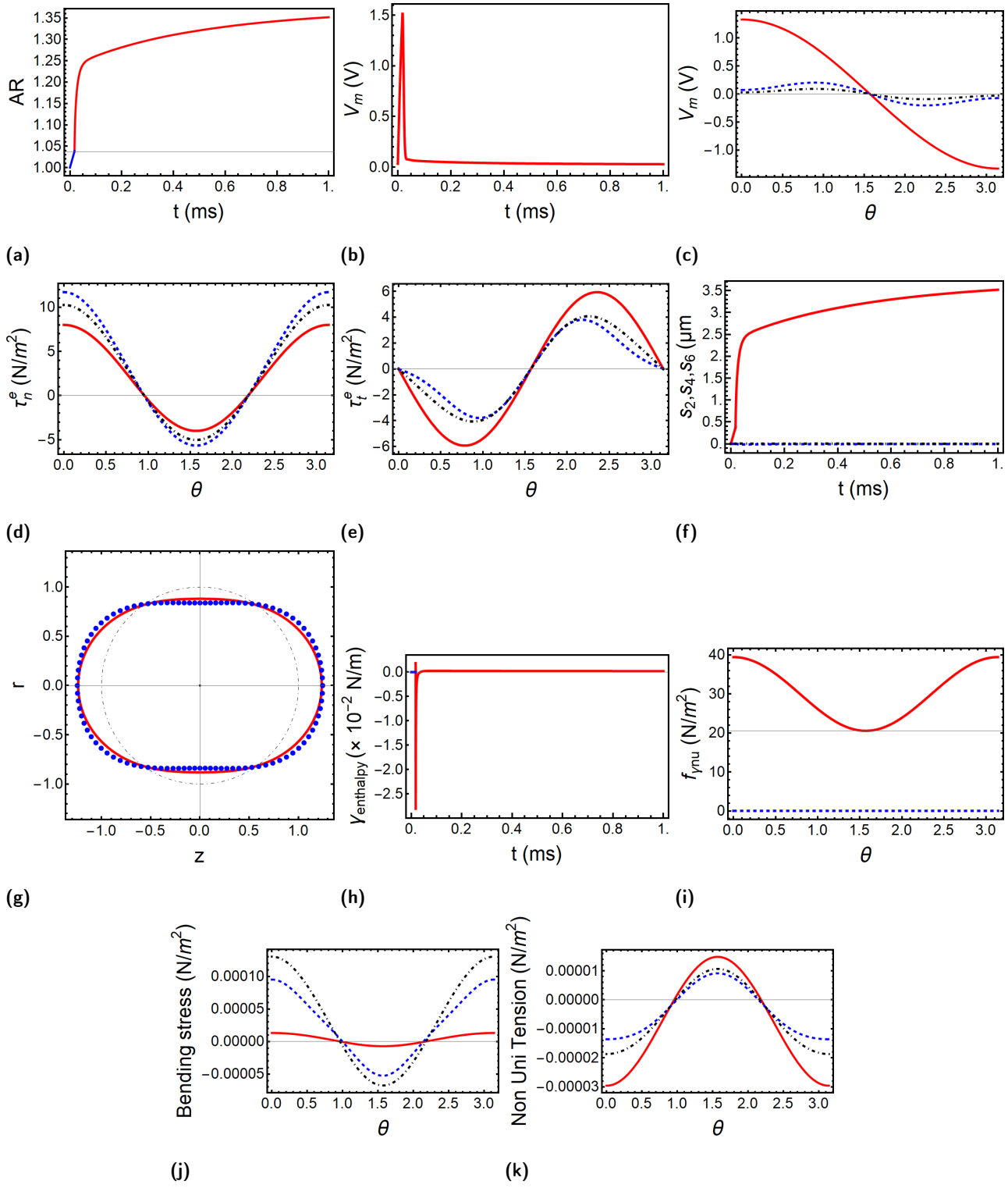

Fig. S16 Plots for $\beta > 1$, low salt, E=1.5 kV/cm, porated: (a) AR vs t plot, (b) V_{mb} vs t, (c) V_{mb} vs θ, $t = \tau_c/2$-red solid, $t = 1.5\tau_c$-blue dashed, $t = t_p$-black dotdashed, (d) Normal electric stress (τ_n^e) vs θ, $t = \tau_c/2$-red solid, $t = 1.5\tau_c$ -blue dashed, $t = t_p$-black dotdashed, (e) Tangential electric stress (τ_t^e) vs θ, $t = \tau_c/2$-red Solid, $t = 1.5\tau_c$-blue dashed, $t = t_p$-black dotdashed, (f) s_2, s_4, s_6 vs t, s_2-red solid, s_4-blue dashed, s_6-black dotdashed, (g) r vs z circle- black dotdashed, model prediction-red solid, experimental - blue dots (h) $\gamma_{enthalpy}$ vs t plot, (i) Capillary stress due to non uniform tension ($f_{\gamma nu}$) vs t, (j) Bending stress vs θ, $t = \tau_c/2$-red solid, $t = 1.5\tau_c$-blue dashed, $t = t_p$-black dotdashed, (k) Non Uniform tension (τ_n^e) vs θ, $t = \tau_c/2$-red solid, $t = 1.5\tau_c$ -blue dashed, $t = t_p$-black dotdashed.

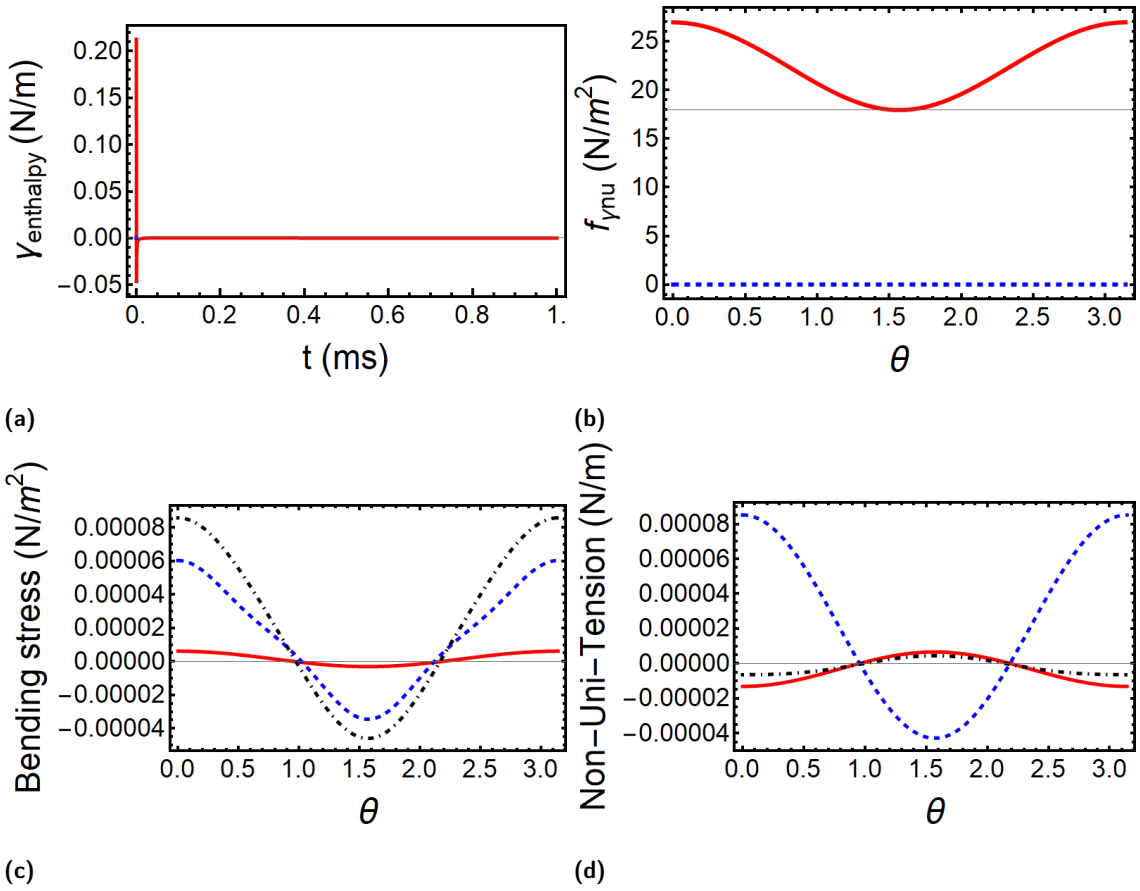

Fig. S17 Plots for $\beta > 1$, high salt, E=1 kV/cm, porated: (a) $\gamma_{enthalpy}$ vs t plot, (b) Capillary stress due to non uniform tension ($f_{\gamma nu}$) vs t, (c) Bending stress vs θ, $t = \tau_c/2$-red solid, $t = 1.5\tau_c$-blue dashed, $t = t_p$-black dotdashed, (d) Non Uniform tension (τ_n^e) vs θ, $t = \tau_c/2$-red solid, $t = 1.5\tau_c$ -blue dashed, $t = t_p$-black dotdashed.

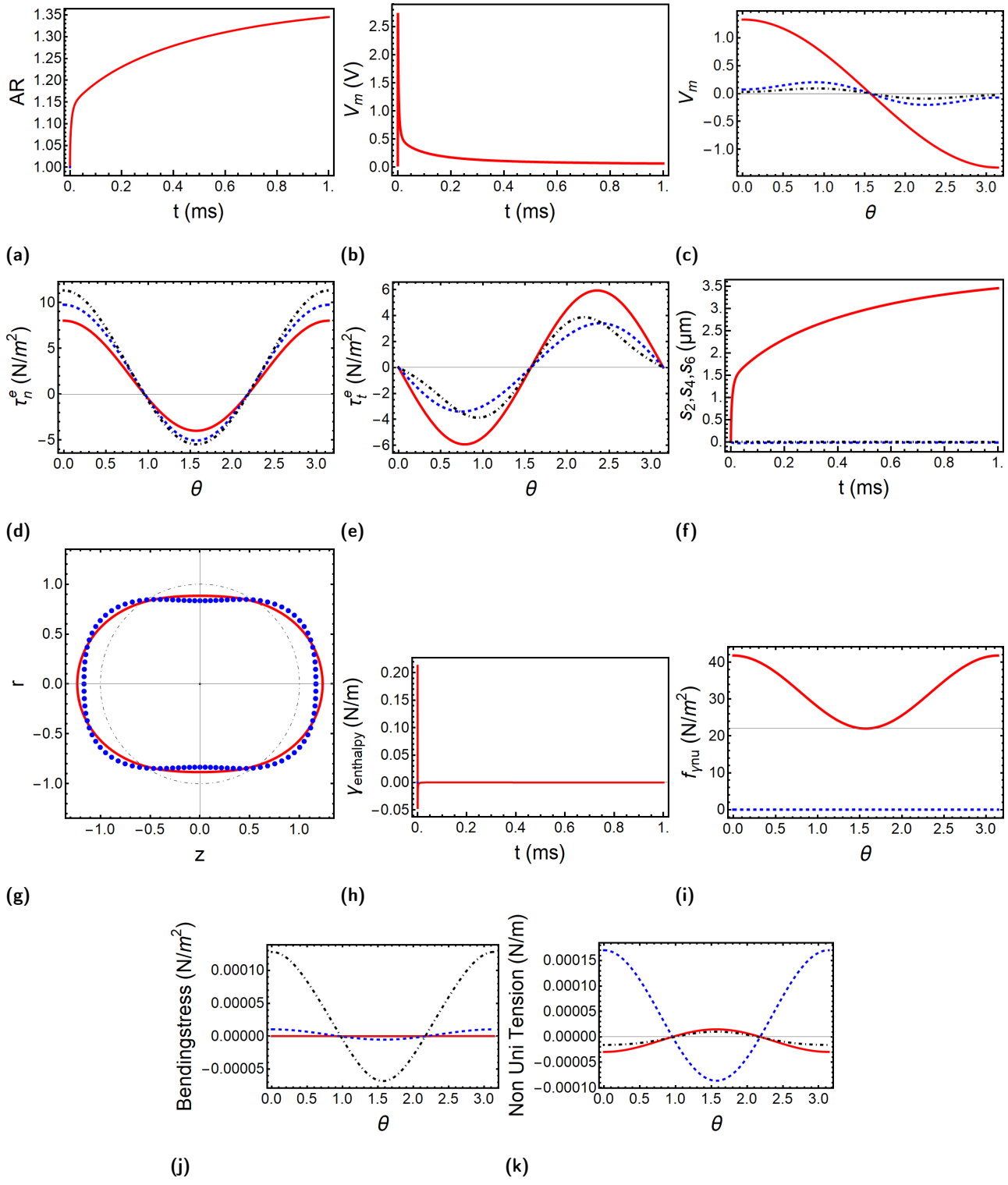

Fig. S18 Plots for $\beta > 1$, high salt, E=1.5 kV/cm, porated: (a) AR vs t plot, (b) V_{mb} vs t, (c) V_{mb} vs θ, $t = \tau_c/2$-red solid, $t = 1.5\tau_c$-blue dashed, $t = t_p$-black dotdashed, (d) Normal electric stress (τ_n^e) vs θ, $t = \tau_c/2$-red solid, $t = 1.5\tau_c$ -blue dashed, $t = t_p$-black dotdashed, (e) Tangential electric stress (τ_t^e) vs θ, $t = \tau_c/2$-red Solid, $t = 1.5\tau_c$-blue dashed, $t = t_p$-black dotdashed, (f) s_2, s_4, s_6 vs t, s_2-red solid, s_4-blue dashed, s_6-black dotdashed, (g) r vs z circle- black dotdashed, model prediction-red solid, experimental - blue dots, (h) $\gamma_{enthalpy}$ vs t plot, (i) Capillary stress due to non uniform tension ($f_{\gamma nu}$) vs t, (j) Bending stress vs θ, $t = \tau_c/2$-red solid, $t = 1.5\tau_c$-blue dashed, $t = t_p$-black dotdashed, (k) Non Uniform tension (τ_n^e) vs θ, $t = \tau_c/2$-red solid, $t = 1.5\tau_c$ -blue dashed, $t = t_p$-black dotdashed.

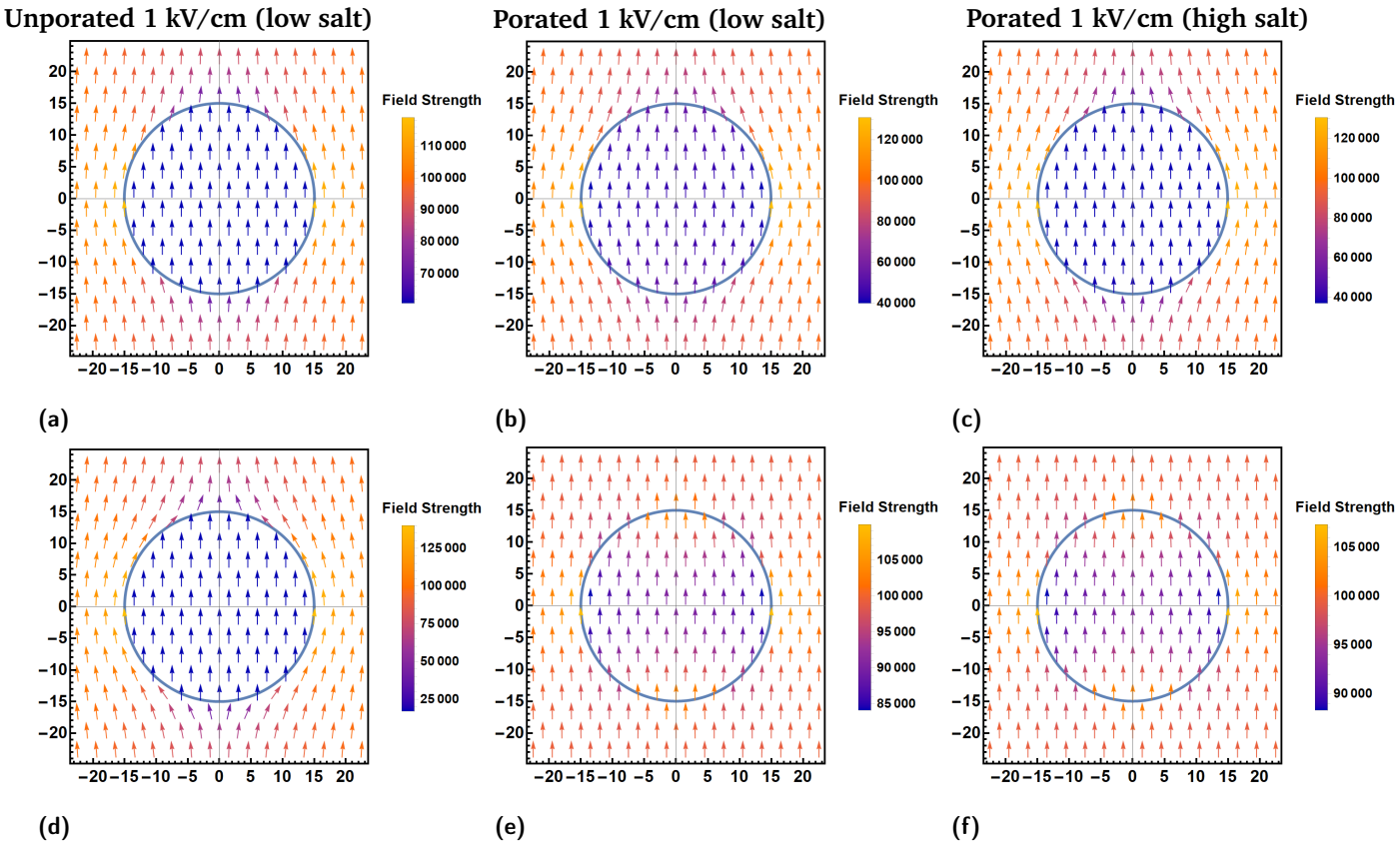

Fig. S19 Electric field (V/m) distribution for $\beta = 1$, (a) and (d) 1kv unporated, (b) and (e) 1 kV/cm porated, all at low salt (c) and (f) 1 kV/cm porated at high salt (first-row at $t = \tau_c$, second-row at $t = t_p$). Electric field in the direction of the arrow (bottom to top).

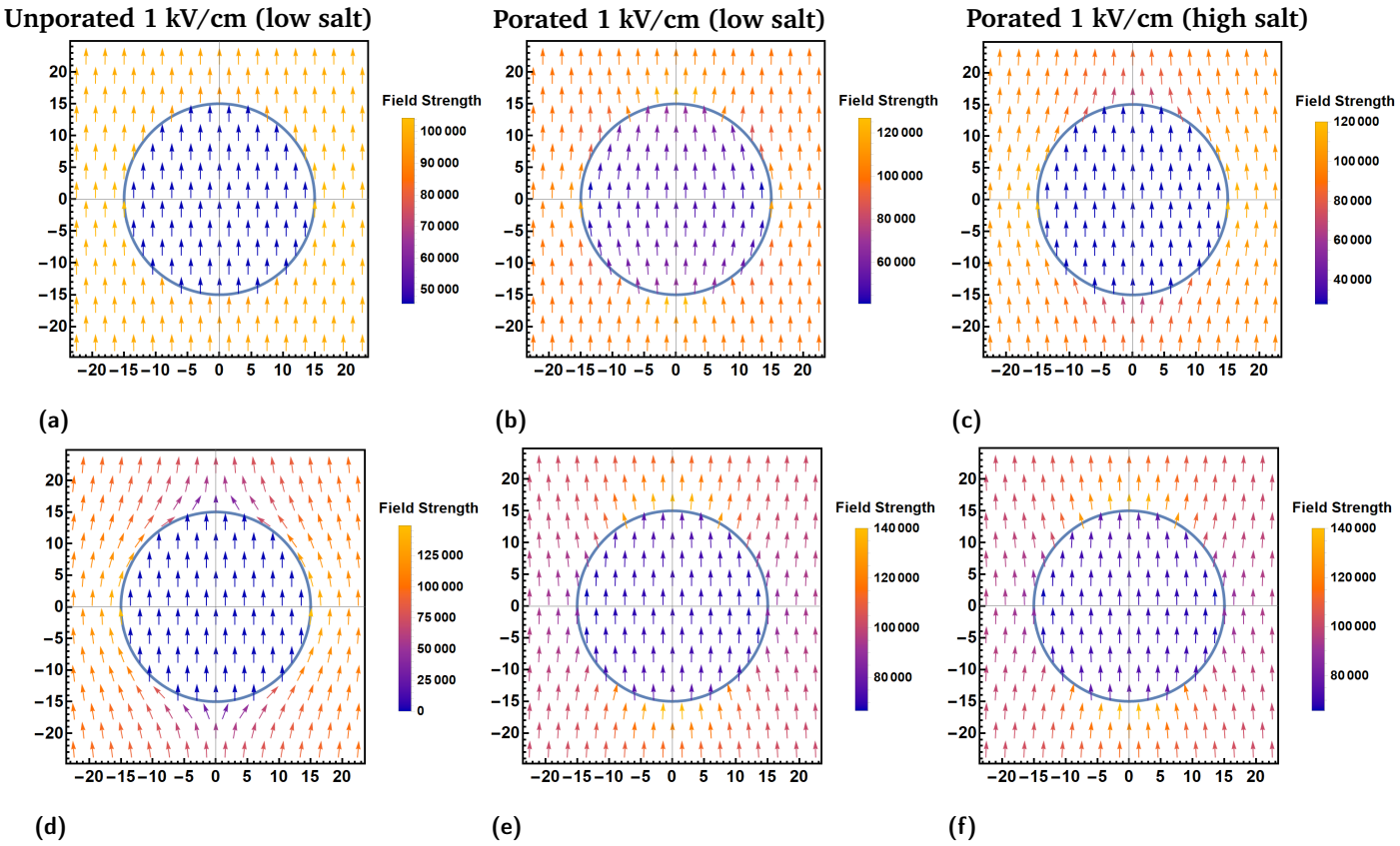

Fig. S20 Electric field (V/m) distribution for $\beta > 1$, (a) and (d) 1 kV/cm unporated, (b) and (e) 1 kV/cm porated, all at low salt (c) and (f) 1 kV/cm porated at high salt (first-row at $t = \tau_c$, second-row at $t = t_p$). Electric field in the direction of the arrow (bottom to top).

Notes and references

1 M. Maoyafikuddin, S. V. Kulkarni and R. M. Thaokar, *ACS Omega*, 2025.

2 K. A. Riske and R. Dimova, *Biophysical journal*, 2006, **91**, 1778–1786.

3 P. F. Salipante and P. M. Vlahovska, *Soft matter*, 2014, **10**, 3386–3393.